

Sequential Decision-Making in a Variable Environment: Modeling Elk Movement in Yellowstone National Park as a Dynamic Game

Erik G. Noonburg¹, Lora A. Newman², Mark Lewis³
Robert L. Crabtree⁴, Alexei B. Potapov³

¹Corresponding author. Centre for Mathematical Biology
Department of Biological Sciences, University of Alberta,
Edmonton, Alberta T6G 2E9, Canada

Current address: Department of Biological Sciences
Florida Atlantic University
2912 College Ave., Davie, FL 33314 U.S.A.
email: enoonbur@fau.edu, tel.: (954) 236-1303

²9501 Chatterleigh Drive, Richmond, VA 23233 U.S.A.

³ Centre for Mathematical Biology,
Department of Mathematical and Statistical Sciences,
University of Alberta, Edmonton, Alberta T6G 2G1, Canada

⁴Yellowstone Ecological Research Center,
2048 Analysis Drive, Suite B, Bozeman, MT 59718, U.S.A.

Key-words: dynamic programming, foraging theory, game theory,
Cervus elaphus, Yellowstone National Park

September 27, 2006

Abstract

We develop a suite of models with varying complexity to predict elk movement behavior during the winter on the Northern Range of Yellowstone National Park (YNP). The models range from a simple representation of optimal patch choice to a dynamic game, and we show how the underlying theory in each is related by the presence or absence of state- and frequency-dependence. We compare predictions from each of the models for three variables that are of basic and applied interest: elk survival, aggregation, and use of habitat outside YNP. Our results suggest that despite low overall forage depletion in the winter, frequency-dependence is crucial to the predictions for elk movement and distribution. Furthermore, frequency-dependence interacts with mass-dependence in the predicted outcome of elk decision-making. We use these results to show how models that treat single movement decisions in isolation from the seasonal sequence of decisions are insufficient to capture landscape-scale behavior.

1 Introduction

Ecologists rely on increasingly sophisticated models to predict the movement behavior and distribution of animals (reviewed in Grimm, 1999; Grimm & Railsback, 2005). These models range from individual-based simulations in which foragers follow predefined rules in response to environmental variation (e.g., Revilla et al., 2004; Jager et al., 2006), to relatively complicated algorithms that seek adaptive foraging strategies for individuals in a population of competitors (e.g., Huse & Giske, 1998; Alonzo & Mangel, 2001; Heinz & Strand, 2006). The development of these models has stimulated two related questions. First, what degree of model complexity is necessary to explain observed distribution and movement patterns of animals (Stephens et al., 2002; Jepsen et al., 2005)? Second, what is the relationship between these models and more basic ecological theory (Grimm, 1999)?

The link between individual-based models and basic optimal foraging theory is of particular interest to behavioral and landscape ecologists. Evolutionary ecologists have established a long tradition of analyzing foraging behavior as the outcome of adaptive processes at the individual level (Stephens & Krebs, 1986) and have developed a suite of theoretical constructs, such as optimal patch choice, residence time, and giving-up density (Emlen, 1966; MacArthur & Pianka, 1966; Charnov, 1976; Brown, 1988), the ideal free distribution (Fretwell & Lucas, 1970; Sutherland, 1983), and density dependent habitat selection theory (Morris, 2003; Jonzén et al., 2004). However, it is typically difficult to scale up the results of the basic models to guide the development and understanding of more complex landscape-level models (Lima & Zollner, 1996; Bowler & Benton, 2005). This difficulty arises from the necessity to consider the fitness value of a sequence of decisions made by an individual in an environment that varies across large spatial and temporal scales. More specifically, how is the outcome of a single optimal movement decision

(e.g., choosing the best neighboring grid cell at each time step in an individual-based population simulation) related to the sequence of decisions optimized as a whole? Similarly, how is the distribution at each time step predicted by individual-based model related to the ideal free distribution?

We address the issues of model complexity and the link between behavioral ecology and landscape models in the context of a particular system, winter movement behavior of elk (*Cervus elaphus*) on the Northern Range of Yellowstone National Park (YNP), U.S.A. Houston (1982) provides a detailed description of the natural system and its management history (see National Research Council (2002) for more recent discussion). During the winter, elk move from high elevation areas on the Northern Range to lower elevations inside and outside the park. Mobility and foraging can be severely limited by snow accumulation (Parker et al., 1984; Sweeney & Sweeney, 1984; Coughenour, 1994) and, because there is no regrowth of forage during the winter, an individual elk must contend with a dynamic pattern of competition from other grazers. A winter hunt imposes substantial mortality risk outside the park, and recent studies have suggested that the reintroduction of wolves to YNP in 1995 may have initiated a trophic cascade (Ripple & Beschta, 2004; Creel et al., 2005; Fortin et al., 2005a). Because this herd is closely intertwined with the local economy and management of YNP, predicting the movement of the elk is of applied as well as basic ecological interest (National Research Council, 2002).

We model landscape scale movement in the framework of a state-dependent game between members of the herd and optimize individual elk foraging decisions with the dynamic programming algorithm. The general technique has been used in the ecological literature to predict animal distributions (e.g., Alonzo & Mangel, 2001); however, our model is unique in this context in that we treat an individual forager's current location as a state variable. Although this feature is not conceptually novel, it is critical to predicting landscape scale movement of grazers

because the large distance between potential foraging patches makes makes current location an important determinant of the payoff from moving to another location. Elk foraging on the Northern Range of YNP has been the subject of study at the level of small scale adaptive foraging decisions and landscape scale patterns (e.g., Turner et al., 1993, 1994; Fortin et al., 2005*a,b*). Here, we place two simpler models of patch choice, state-dependent optimization and the ideal free distribution (IFD), in the common framework of the state-dependent game to address the link between adaptive behavior at the level of individual foragers and landscape scale patterns. We use each model to predict three specific features of elk winter movement that are of basic and applied interest: aggregation, use of habitat outside YNP, and survival through the winter. We ask not only what we would miss with the simpler optimal patch choice and IFD models, but also how state and frequency-dependent mechanisms interact in the more complex state-dependent game model to generate the predicted landscape level patterns.

2 Methods

The model framework consists of two distinct parts: 1) a representation of the natural system including elk energetics, snow accumulation, and forage availability; and 2) an optimization procedure to calculate the movement decisions that maximize individual fitness given the natural system. We use four variants of the optimization procedure to find sequences of movement decisions that maximize different fitness measures that are related within the framework of the full state-dependent game model. With the results of each of the four optimizations, we simulate the herd behavior in identical environmental conditions so we can compare the predicted herd movement and survival.

The optimizations find the sequence of moves between patches for an individual elk that starts the winter in any one of the patches. The four model variants that we consider incorporate

different combinations of state- and frequency-dependence in the optimization (summarized in Table 1). The optimal behavior in all of the models depends on an individual's location at a given time step, which influences the movement cost to reach another patch. However, we conduct the optimization with and without individual mass (a measure of physiological condition) as a dynamic state variable. Similarly, we conduct the optimization with and without the influence of forage competition from the herd (frequency-dependence).

We selected mass- and frequency-dependence to include in our analysis for two reasons. First, although forage is depleted by the herd and survival and future reproductive success depend on individual mass, it is not obvious to what degree either influences behavior at the landscape scale. More specifically, grazers typically remove less than 10% of primary production on Yellowstone's Northern Range (Houston, 1982), and winter forage availability may be primarily determined by snow accumulation. Similarly, overall winter foraging conditions are poor, and a strategy in which an individual simply maximizes ingestion regardless of current mass is a reasonable behavior to hypothesize. The second reason is that, as we show below, removal of physiological state- and frequency-dependence allows us to relate the full state-dependent game to simpler models of optimal patch choice.

In the following section we describe the natural system, which is the common environment in which we conduct the optimizations. Next, we detail the four optimization procedures for the model variants.

2.1 Elk on Yellowstone's Northern Range

Yellowstone's Northern Range consists of approximately 100,000 ha along the Yellowstone, Gardiner, and Lamar River drainages (Houston, 1982). We consider the area defined by the 68 ungulate count units used by the National Park Service for elk population censuses (Figure 1);

about 17% of this area is outside the park boundary but can contain half of the herd during some winters. We use the count units as patches in the model. Each count unit encompasses considerable environmental heterogeneity; however, we are primarily interested in capturing large scale seasonal movement, which can cover tens of kilometers, rather than daily movement patterns, e.g., between grazing and resting habitats. Furthermore, use of the count units is intended to facilitate future comparisons with winter census data.

The model representation of environmental variation involves substantial simplification of the natural system. The spatial relationships between patches appear only as the distances between the centers of mass of the count units. We use a simplification of Biggs's (1995) snow model to generate snow water equivalent in each patch at each time step. The snow model incorporates two variables: elevation, and an increasing snow gradient from west to east (Appendix A.1). We assume an intermediate forage density per unit area to obtain initial forage abundance in each patch; hence, total forage varies only with patch area (Appendix A.2).

The major predators of elk inside the park are wolves, bears, cougars, and coyotes, whereas human hunting is the primary source of predation outside the park (Houston 1982, NRC 2002). Our goal is to establish predictions for elk movement prior to wolf reintroduction; hence, we exclude wolves as a source of predation. In general, we expect predation within the park to vary with habitat type at a smaller scale than the ungulate count units. Furthermore, mortality from predators other than wolves is typically low (Houston, 1982). Hence, the primary consideration is the difference in predation risk between patches inside and outside the park. With this in mind, we ignore predation inside the park and include human hunting as the only source of predation. For the sake of simplicity, we assume a constant probability of hunting mortality in patches outside the park (Appendix A.3).

We distinguish three age/sex classes of elk: bulls, cows, and calves, which differ in some

parameter values (Table 2, Appendix A.4). We evaluate movement strategies during a 20-week winter. Physiological state and survival in a given patch during week t depend on four variables: distance traveled, snow, forage density, and mortality risk from hunting. We model physiological state as the mass of an individual. Change in mass (Δm) depends on the difference between energy gained from foraging (E_{gain}) and maintenance and travel costs (E_{maint} and E_{travel}):

$$\Delta m = \eta (E_{gain} - E_{maint} - E_{travel}), \quad (1)$$

where η is the conversion factor from energy to mass.

We assume maintenance depends only on body mass according to the standard allometric function

$$E_{maint} = \mu m^{3/4} \quad (2)$$

with constant μ . Travel costs increase with body mass, distance traveled, and snow depth. We use the empirically derived function from Parker et al. (1984):

$$E_{travel} = 2.97Km^{0.34} \left(1 + 0.71(D_{p,t}/H_i)e^{0.0191(D_{p,t}/H_i)} \right), \quad (3)$$

where K is the distance traveled (between the centers of the patches and regular foraging movement; see Appendix A.4), H_i is brisket height, and $D_{p,t}$ is snow depth in patch p at time t (Appendix A.1). (In our application of the function measured by Parker et al. (1984), we assume the average value for snow density and that elk sinking depth is equal to snow depth.)

We assume energy gain from foraging (E_{gain}) depends on an individual's age/sex class but not on body mass. Snow accumulation and forage depletion reduce the ingestion rate from its physiological maximum, $I_{max,i}$. We assume ingestion rate for age/sex class i depends on the variable that has the greater effect:

$$I_i(t) = I_{max,i} (1 - \max(B_{snow}(t), B_{forage}(t))). \quad (4)$$

$B_{snow}(t)$ is the fractional reduction in the maximum ingestion rate caused by snow depth at week t . Similarly, $B_{forage}(t)$ is the fractional reduction caused by forage depletion at time t .

Snow depth and density influence elk foraging ability. We measure the combined effect with snow water equivalent ($SW E_{p,t}$; see Appendix A.1). We use the following function for $B_{snow}(t)$:

$$B_{snow}(t) = \begin{cases} 0 & SW E_{p,t} < SW E_{low} \\ \frac{SW E_{p,t} - SW E_{low}}{SW E_{high} - SW E_{low}} & SW E_{low} \leq SW E_{p,t} \leq SW E_{high} \\ 1 & SW E_{p,t} > SW E_{high} \end{cases} \quad (5)$$

where $SW E_{high}$ and $SW E_{low}$ are threshold snow levels (see Turner et al., 1994). Between the lower and upper thresholds, increasing snow water equivalent causes a linear decrease in the ingestion rate.

We employ a similar linear function for $B_{forage}(t)$, with the additional constraint that a fraction r of forage initially present in each patch is unavailable due to trampling and packing of snow by foraging elk (Turner et al., 1994). $B_{forage}(t)$ increases from 0 to 1 as elk deplete the forage in a patch ($f_p(t)$) toward the minimum abundance ($r f_p(0)$):

$$B_{forage}(t) = 1 - \frac{f_p(t) - r f_p(0)}{(1 - r) f_p(0)}. \quad (6)$$

Although we model movement decisions and snow accumulation at discrete, one-week intervals, we model forage depletion continuously within each time step. This allows us to calculate the effect of competition on the foraging success of an individual during a week. The rate of change in forage abundance at any time t is

$$\frac{df_p(t)}{dt} = - \sum_i N_{i,p}(t) I_i(t), \quad (7)$$

where $N_{i,p}(t)$ is the number of elk of age/sex class i in patch p , and $I_i(t)$ is specified by Eq. 4.

Energy gained from foraging by an individual is ingestion integrated over the one-week time step:

$$E_{gain} = \varepsilon \int_t^{t+1} I_i(x) dx, \quad (8)$$

where ε is the coefficient for conversion of forage mass to energy.

We calculate the amount of forage consumed by elk in each patch during a week to obtain the forage abundance at the beginning of the next week:

$$f_p(t+1) = f_p(t) - \sum_i N_{i,p}(t) \int_t^{t+1} I_i(x) dx. \quad (9)$$

We model two sources of mortality, starvation and human hunting. An individual of age/sex class i dies of starvation if its mass falls below a critical value, $m_{crit,i}$. We assume a constant probability of death from hunters in patches outside the park (Appendix A.3). We denote the probability that an elk of age/sex class i survives week t as $S_i(t)$.

2.2 Optimization model variants

The representation of the natural system in the previous section determines the forage consumption and survival of elk given the movement decisions of each individual in the herd. In the next four sections we describe the different optimization models that we apply to generate individual movement decisions. We assume elk have complete information about the difference in predation risk between patches inside and outside YNP. (This is consistent with anecdotal evidence; however, it is unknown whether elk have learned that areas outside the park are risky or simply use local cues such as odor to avoid hunters.) The optimization models differ in their assumptions regarding the use of information about foraging conditions.

In all of the models we assume calves must move with their mothers. Hence the three age/sex classes are cow-calf pairs, cows without calves, and bulls, and we treat a cow-calf pair as an individual in the optimizations.

Model 1. Base model

In our simplest model we calculate the optimal movement decision at each time step for an elk with mass equal to the initial average for its age/sex class and no competition. We maximize the

immediate payoff for an individual of age/sex class i (φ_i), which we define to be the product of survival and change in mass from t to $t + 1$:

$$\varphi_i = \Delta m_i S_i(t). \quad (10)$$

Survival probability, $S_i(t)$, depends only on the patch that the individual selects at week t . For calf-cow pairs, the immediate payoff (φ_{cc}) is modified to include calf foraging success:

$$\varphi_{cc} = \Delta m_{cow} S_{cow}(t) + q \Delta m_{calf} S_{calf}(t), \quad (11)$$

where the parameter q weights the contribution of the calf to its mother's immediate payoff (we set $q = 1$ in our simulations.)

We conduct the optimization at each week using the initial average mass at the beginning of the winter, so that mass is not a dynamic state variable. Hence, an individual does not sacrifice its immediate payoff for a potentially greater payoff over the entire winter. Furthermore, we perform the optimization in the virgin environment, as if only snow accumulation limited ingestion. In the optimization, this implies that Δm_i is calculated with $f_p(t) = f_p(0)$ throughout each time step and over the entire winter.

This model is obviously a simplistic representation of elk decision-making. The optimization does not account for the effect of mass change in the current time step on the outcome of future decisions (contrast with model 3). The optimization also does not account for forage depletion by the herd. This model merely predicts the sequence of patches with inherently high quality (low snow, weighted by predation risk) for an individual starting in any patch. The model reduces the problem to basic optimal patch choice at each time step.

Model 2. Ideal free distribution with travel costs

We introduce frequency-dependence to the base model by maximizing the immediate payoff (φ_i) to each individual given the forage depletion by competitors. Forage depletion by competitors

alters the immediate payoff by reducing the ingestion rate and therefore Δm during a week. Forage abundance and ingestion rate decline continuously throughout the one-week time step (Eqs 7-8). By adding this effect to the optimization in the base model we obtain an evolutionary stable strategy (ESS) at each time step. The result is an ideal free distribution during each week, where the payoff includes travel costs.

We find the ESS at each week using an iterative procedure (described in greater detail for model 4, below). The technique involves two steps. First, we find the movement decision that maximizes the immediate payoff for an individual in any patch, given the declining food abundance in each patch during the week ($\frac{df_p(t)}{dt} = 0$ in the first iteration). Next, we calculate the resulting ingestion rate for an individual in each patch given the number of elk that move to that patch. We repeat these two steps, each time using the immediate fitness in the first step that results from the ingestion rate calculated in the second step of the previous iteration.

Model 3. Mass-dependent optimization

We add mass-dependence to the optimization in the base model using the general state-dependent dynamic programming algorithm (Mangel & Clark, 1988). This model variant maximizes the product of survival through the entire winter and the terminal fitness function, $\Phi(m(T))$, which is an increasing function of mass at the end of winter. An individual's state at time step t now consists of its mass ($m(t)$) as well as its location (patch p). We refer to the product of over-winter survival and terminal fitness as the net payoff. In this model an individual may make a movement decision in any particular week with less than maximum immediate payoff in order to obtain a greater net payoff.

At each time step, we find the move from patch p to any other patch p' (including stay in the

same patch) that satisfies

$$F(m, p, t) = \max \left(\Phi(m(T)) \prod_t^T S(t) \right), \quad (12)$$

where the maximization is over all p' at the current time step t , and both $m(T)$ and $S(t)$ depend on p' . The dynamic programming algorithm works backward in time to find $F(m, p, t - 1)$ as a function of $F(m, p, t)$. At the end of winter ($t = T$), by definition

$$F(m, p, T) = \Phi(m(T)) \quad (13)$$

for all p . Next, we proceed one time step backward to $t = T - 1$. Expected fitness for each decision is a function of change in mass, Δm , and the probability of survival in the current patch, $S(p)$:

$$F(m, p, T - 1) = \max_{p'} S(p) F(m + \Delta m, p', T). \quad (14)$$

We proceed in an identical fashion to find $F(m, p, T - 2)$ using the values of $F(m, p, T - 1)$ for all m and p :

$$F(m, p, T - 2) = \max_{p'} S(p) F(m + \Delta m, p', T - 1). \quad (15)$$

The backward iteration continues until $t = 0$.

The optimization is modified somewhat for calves. We assume a calf must follow its mother throughout the winter, and that the cow's fitness increases with calf survival and mass at the end of the winter. We treat a calf-cow pair as an individual in the optimization, with terminal fitness equal to the sum of terminal fitnesses of each pair member. Calf terminal fitness is weighted by the parameter q (see Base model, above). Calf-cow state has three components: cow mass (m_c), calf mass (m_j), and location (p). Hence, terminal fitness is

$$F(m_c, m_j, p, T) = \Phi(m_c) + q\Phi(m_j), \quad (16)$$

and the general dynamic programming equation for calf-cow pairs is

$$F(m_c, m_j, p, t - 1) = \max_{p'} S(p) F(m_c + \Delta m_c, m_j + \Delta m_j, p', t). \quad (17)$$

The dynamic programming algorithm requires discretization of the state variables. An elk's location is discretized by the patches, p . We discretize mass into 10 (calves) or 100 (cows and bulls) bins of equal size between maximum and minimum masses (Table 2), where the minimum mass is the starvation threshold.

Terminal fitness, $\Phi(m(T))$, represents future survival and reproductive success of an individual elk. In general, we expect terminal fitness to be an increasing function of mass. The particular shape of this function determines the priority given to mass at the end of winter relative to avoiding predation risk, but we do not have empirical information to specify the prioritization. We adopt a generic function which can take a variety of shapes depending on the value of a single parameter, a . To simplify notation, we let \hat{m} be mass expressed as a fraction of the range of values taken by m in the dynamic programming algorithm: $\hat{m} = \frac{m - m_{crit}}{m_{max} - m_{crit}}$, where m_{crit} is the starvation threshold and m_{max} is the maximum mass. We define terminal fitness as

$$\Phi(m) = \begin{cases} 0 & \hat{m} \leq 0 \\ \frac{a\hat{m}}{a-1+\hat{m}} & \hat{m} > 0 \end{cases} \quad (18)$$

For $a = 1$, $\Phi(m)$ is a step function that assigns value 0 to starvation and 1 to survival, regardless of the particular value of mass. In this case, expected terminal fitness is simply the probability of survival, and the optimization gives priority to avoiding predation until an individual approaches the critical mass for starvation. As a increases, $\Phi(m)$ approaches a linear function and increasing priority is given to maintaining mass relative to avoiding predation. We set $a = 1.05$, which gives an intermediate tradeoff between mass and predation risk.

Model 4. Dynamic game

The full dynamic game incorporates frequency- and mass-dependence in the optimization of elk movement behavior. The algorithm consists of iteration of two steps, optimization and frequency-dependent feedback (see, e.g., Mangel & Clark [1988, pages 259-270] for a general

description of the procedure) to find an ESS. In the optimization we use the dynamic programming algorithm to find the state-dependent decisions that maximize fitness in a given environment. In the second step we predict the herd distribution and forage depletion throughout the winter assuming that every individual follows the optimal behavior. This step generates the temporal sequence of foraging payoffs in each patch for the optimization in the next iteration of the dynamic game algorithm. The optimal strategy is the sequence of decisions that maximizes net fitness (as in model 3) given the behavior of every other individual (as in model 2).

The first iteration predicts the best response by an individual to the virgin environment, i.e., the optimal strategy in the absence of competitors. Repeated iterations find the best response to the best response, i.e., the optimal strategy for an individual given the forage depletion by the herd predicted in the previous iteration. If the iterative procedure converges to a single set of movement decisions, the result is an ESS. However, this basic iterative procedure does not necessarily converge to an ESS, even if one exists. Indeed, our application of the state dependent game algorithm typically resulted in oscillations among multiple strategies.

McNamara et al. (1997) suggest a general technique to prevent the algorithm from becoming trapped in oscillations, as well as conditions for convergence to an ESS. Their technique incorporates “error” in the decision-making process, such that individuals do not always opt for the patch with the highest payoff. Instead, individuals make sub-optimal decisions with probabilities that decrease as the difference in fitness payoff between sub-optimal and optimal decisions increases. An individual is equally likely to move to multiple patches with the same payoff, i.e., we allow mixed strategies.

We develop a novel error function which represents the decision-making process with a simple statistical model of payoff estimation. For an individual with a given state at time t , the optimal decision is to move to the patch with the highest expected value of future reproductive success.

Each potential move from patch p to p' can therefore be ranked by its value of $F(m + \Delta m, p', t + 1)$. We assume that an individual assesses each possible move with some error such that the distribution of estimated patch values is Gaussian with mean $\xi_p = F(m + \Delta m, p, t + 1)$ and variance σ_p . The probability of moving to any patch is the probability that its estimated value is greater than the estimated value for any other patch. If $g_p(x)$ is the distribution of the estimate for patch p , the probability that the estimate for patch 1, for instance, is greater than the estimates for all other patches 2-68 is

$$P_1 = \int_{-\infty}^{\infty} dx_1 \int_{-\infty}^{x_1} dx_2 \dots \int_{-\infty}^{x_1} dx_{68} g_1(x_1) g_2(x_2) \dots g_{68}(x_{68}). \quad (19)$$

An equivalent expression can be obtained for each patch p .

Given our assumption that all g_p are Gaussian, if $h(x)$ is $N(0, 1)$,

$$g_p(x) = \frac{1}{\sigma_p} h\left(\frac{x - \xi_p}{\sigma_p}\right), \quad (20)$$

and we can rewrite Eq. 19 as

$$P_1 = \int_{-\infty}^{\infty} h\left(\frac{x_1 - \xi_1}{\sigma_1}\right) H\left(\frac{x_1 - \xi_2}{\sigma_1}\right) \dots H\left(\frac{x_1 - \xi_{68}}{\sigma_{68}}\right) dx_1 \quad (21)$$

where $H(x)$ is the cumulative distribution function for $h(x)$.

We make the following simplification to Eq. 21 to facilitate the numerical calculations in our dynamic game model. Instead of integrating over the entire range of x_p , we approximate P_p as the probability that estimates for all other patches are less than the mean ξ_p . In this case,

$$P_1 \approx H\left(\frac{\xi_1 - \xi_2}{\sigma_2}\right) H\left(\frac{\xi_1 - \xi_3}{\sigma_3}\right) \dots H\left(\frac{\xi_1 - \xi_{68}}{\sigma_{68}}\right) \quad (22)$$

In all of our solutions we assume constant variance ($\sigma_p = \sigma$) for all 68 patches.

We approximate the ESS by using the minimum error (i.e., we minimize the probability of moving to sub-optimal patches) for which the algorithm converges. We found this minimum

($\sigma = 0.0001$) by trial and error. We present results after 500 iterations; in all cases the difference between successive iterations decreased rapidly enough to assure convergence to an ESS (McNamara et al., 1997).

2.3 Model implementation

The optimization models generate tables of movement probabilities for every combination of mass, patch, time, and age/sex class. We predict the behavior and survival of the herd using these probabilities in the forward projection described above (sec. 2.1). In all four models, the forward projection employs the full description of elk physiology. For instance, in model 1, we perform the optimization assuming an individual does not use information about its proximity to starvation or the movement of competitors. We then predict the mass dynamics and survival of every individual in a herd that is competing for forage using the optimal movement decisions. We therefore obtain the predicted performance of an identical herd using four different levels of decision-making capability.

We start every forward iteration with 15000 elk (divided among the three age/sex classes, Table 2), which falls within the range of variation in initial winter abundance for this herd (NRC, 2002). In the absence of detailed empirical information regarding the initial spatial distribution of the herd, we make the simplest assumption that elk begin evenly distributed over the area inside the park. We further assume that within each age/sex class, initial mass follows a truncated normal distribution scaled such that the starvation threshold is three standard deviations below the average initial mass, and we set the maximum mass to one standard deviation above the initial average mass.

3 Results

The output from each model is the sequence of moves among patches for every elk, from which we obtain the number of elk in each patch at each time step (Fig. 2). We summarize the results to predict two general features of the movement sequence: the fraction of the herd in patches outside the park, and the coefficient of variation (CV) among patches in number of elk at each time step. The fraction of the herd that is outside the park in a given week corresponds to the level of risk from hunting that elk are willing to accept under the current snow and forage conditions. The coefficient of variation quantifies the aggregation of the herd, i.e., high CV indicates that most elk have moved to only a few patches. We also compare the predicted survival of each age/sex class to the end of the winter as an indication of the viability of the movement strategy generated by each model.

The movement pattern is qualitatively similar in all four models (Fig. 3): elk gradually move to patches with less snow (lower elevation and west) as forage availability decreases and movement costs increase, and elk move outside the park when forage availability outweighs the risk imposed by hunters. The models vary in the suddenness and timing of movement across the park boundary. Models with frequency-dependence predict a more gradual move than models without frequency-dependence. Not surprisingly, models with frequency-dependence also predict lower aggregation throughout the winter. Despite the broad similarity of the movement and distribution patterns, only the full dynamic game (model 4) predicts appreciable calf survival (Table 3).

We obtain a more detailed understanding of the different model predictions by examining the results separated by age/sex class. First, we compare predictions from the models lacking frequency-dependence (Fig. 4). The base model predicts the same movement pattern for all three age/sex classes: gradually increasing aggregation during the first half of the winter followed by a

sudden move to a single patch outside the park where the herd remains for the latter half of the winter. Hence, the best choice based on underlying patch quality (i.e., without forage depletion by competitors or individual mass-dependence) depends on initial location only for the first half of the winter. Subsequently, all individuals select the same patch regardless of where they started.

The addition of mass-dependence delays the move outside slightly and increases aggregation among calf-cow pairs (Fig. 4). The delay is due to the reduction in the value of early foraging, because early mass gain is offset by increasing maintenance and travel costs. Snow accumulation has a greater effect on travel costs for small elk, so consideration of future fitness implied by mass-dependence forces calf-cow pairs to move more rapidly ahead of increasing snow, which causes their early aggregation in low-elevation patches.

Next, we address the effects of considering competition in the optimization (Fig. 5). Frequency-dependence alone makes the move outside the park more gradual and reduces aggregation during the latter half of the winter. These effects are broadly similar across age/sex classes, which indicates that competition influences movement decisions regardless of elk size.

The combination of frequency- and mass-dependence in the full model returns the predicted pattern to an all-or-nothing move across the park boundary, as in the base model; however, the herd is strongly segregated by age/sex class (Fig. 5). Calf-cow pairs move outside the park first, followed by cows, whereas almost all bulls remain inside the park throughout the winter. Furthermore, the full model predicts higher aggregation among calf-cow pairs early in the winter, but not as high as in the model with only mass-dependence. These patterns suggest that calf survival depends on the combination of moving outside the park early in the winter to avoid travel costs imposed by snow, and reduced early aggregation to avoid competition. The former effect arises from mass-dependence (i.e., maximizing future fitness requires moving ahead of snowfall), whereas the latter effect arises from frequency-dependence.

4 Discussion

Comparison of the four models reveals the interaction between mass- and frequency-dependence in the movement pattern predicted by the full state-dependent dynamic game model. In our simulations, the herd consumed less than 4% of the total forage mass present at the beginning of the winter (Table 3). Nevertheless, forage competition is crucial to the predictions of the full model. Removal of frequency-dependence from the full model (model 2 vs. model 4) results in large changes in the timing of movement across the park boundary as well as in calf survival. Similarly, despite overall poor foraging conditions due to snow accumulation, simply minimizing the product of mass loss and predation risk each week (model 3) also results in substantial differences in predicted movement and calf survival relative to the full model. Furthermore, the effects of either mass- or frequency-dependence depend on the presence of the other in the model. These results demonstrate that the predictions of the full state-dependent game model can not be captured by simulating elk movement with simpler behavioral rules (e.g., move out of high-elevation patches as snow depth increases).

Elk censuses on Yellowstone's Northern Range are generally conducted only once each winter and do not permit rigorous comparison with the weekly predictions for herd distribution and movement in our model. However, two general features of elk movement patterns predicted by the full model suggest avenues for future testing. First, the difference between movement of cow-calf pairs and cows without calves, and the high calf mortality predicted by the simpler models 1-3, suggest that cows may have to sacrifice their own foraging success to accommodate calf foraging. Second, the model predicts a general trend in which cow-calf pairs move outside the park first, followed by cows without calves and finally bulls. This pattern reflects the tradeoff between the risk of hunting outside the park and foraging ability in snow, which varies with elk height. These

broad characteristics of winter movement behavior could be compared to observations of a relatively small number of individuals tracked throughout the winter.

We limited the biological details in the full model to features that are reasonably well described in the literature. The ultimate goal is to incorporate sufficient realism to make predictions that can inform management decisions. However, the model simplifications required for computational feasibility limit our predictions in several areas. For instance, we did not consider elk social interactions other than calf-cow pairing. During the winter, bulls are typically segregated from cows and calves, but adult females and first-year offspring often travel in groups (Houston, 1982). Although our model predicts that cows and calf-cow pairs tend to be aggregated at the scale of the count units even without incorporating more detailed social interactions, simulating larger social groups could influence the outcome, particularly in a model with greater spatial resolution in the patch structure.

The relatively coarse spatial resolution of our model also limits our representation of spatial variability in the habitat. Our results suggest strong selection to move to the two lowest patches in and outside YNP later in the winter, despite competition. However, Houston's (1982) summary of the elk census data suggests that such extreme aggregation does not occur even in severe winters. We hypothesize one mechanism that can alter the degree of aggregation predicted by the dynamic game model: within-patch heterogeneity in forage availability related to small-scale variation in snow. We used a single value of elevation for each patch to capture large-scale differences in snowfall across the Northern Range, but each patch is sufficiently large to contain substantial heterogeneity in snow conditions. Modification of the full model to include a simple representation of this heterogeneity (a fraction of each patch has the snow depth that is predicted for the lowest elevation in the patch) demonstrates that even a small area of relatively high forage availability in otherwise poor quality patches reduces the predicted aggregation considerably

(Fig. 6). Because more food is available inside the park, within-patch heterogeneity delays calf-cow pair movement outside the park, and cows without calves are less likely to make the transition to patches with hunting.

Our state-dependent game model differs from typical rule-based simulation models in that we optimize behavior so as to maximize the product of terminal fitness and the probability of survival through the entire winter, rather than the immediate payoff at each time step. Of our four models, the ideal-free distribution with travel costs (model 2) is closest to a rule-based simulation: movement decisions maximize the immediate payoff at each time step given forage depletion by competitors. The results of model 2 can be compared to the rule-based simulation of elk on Yellowstone's Northern Range developed by Turner et al. (1994), who assumed elk select the patch with the highest immediate payoff from within a relatively small perceptual radius. Turner et al. simulated a variety of scenarios, but typically obtained greater calf survival and lower adult survival than in our model 2. We speculate that small scale habitat heterogeneity accounts for these differences. Turner et al. simulated movement on a habitat map with 1 ha resolution, which allows for considerable variability in forage availability within the count units that we used as patches. This presumably allows adults and calves to access nearby patches with high forage availability, but the narrow perceptual radius prevents long distance moves to avoid local "traps" of low forage availability created by snow or competitors. Not surprisingly, our full model predicts relatively high survival compared to the simulations of Turner et al. (1994).

The ideal free distribution serves as a benchmark for the prediction of grazer distributions (Senft et al., 1987; Coughenour, 1991; Bailey et al., 1996; Farnsworth & Beecham, 1999). Although the IFD may be the outcome of individual foragers following simple behavioral rules (Bernstein et al., 1988, 1991; Farnsworth & Beecham, 1999), the IFD is a static distribution and its calculation for a particular set of environmental conditions does not in general imply any

predictions about the optimal movement of individuals over time. Similarly, the fact that a particular movement rule applied over successive time steps eventually generates an IFD does not imply that the movement rule is an evolutionary stable strategy in a dynamic environment. For instance, in a general treatment of individual-based grazer movement models, Farnsworth & Beecham (1999) suggested that increasing the individual perceptual radius to encompass the entire landscape, such that foragers can move toward distant high-payoff patches, recovers the ideal free distribution. However, moving toward a distant patch will not be successful if competitors deplete that patch first. Instead, the forager may spend all of its time chasing transient peaks in the forage distribution. Maximizing the net payoff at the end of the season given competitor movement and forage depletion requires optimization of the sequence of decisions as a whole, rather than optimization of individual decisions.

Acknowledgements

We thank D. Bennett, H. Beyer, S. Hamilton, M. Hebblewhite, D. McGinnis, E. Merrill, N. Varley, D. Visscher, PJ White, and members of the Lewis lab and Yellowstone Ecological Research Center for helpful discussions. Financial support was provided by NSF Grant DEB-2016588, an NSERC Discovery Grant, and a Canada Research Chair.

A Parameterization and patch characteristics

A.1 Snow

The Biggs (1995) model uses data from five local weather stations and snow courses, as well as elevation, slope, aspect, and east-west location to predict snow water equivalent and snow depth for any location on the Northern Range. We simplify the model to include only elevation and aspect, which explain 90% of the variance in snowfall. The result is the following pair of equations

for snow water equivalent ($SWE_p(t)$) and snow depth ($D_p(t)$) in patch p at week t :

$$\begin{aligned} SWE_{p,t} = & -15.2069 - 5.2805\overline{SWE}_t + 0.001418(\overline{SWE}_t \times ELEV_p) \\ & + 0.006128(WS(t) \times UTMx_p) \end{aligned} \quad (23)$$

and

$$D_p(t) = 1.985SWE_{p,t} + 661.287 \left(1 - \frac{113.315}{SWE_{p,t} + 113.315} \right), \quad (24)$$

where \overline{SWE}_t is the average SWE at week t from the five weather stations in the area, $ELEV_p$ is elevation, and $UTMx_p$ is the east-west coordinate of the center of mass of the patch. For elevation we use the harmonic mean of maximum and minimum elevations in each patch (Ballinger, 1999).

This gives less weight than the arithmetic mean to peak elevations, which elk can avoid.

We used averaged weather station data from 1988, 1989, 1990, 1992, and 1993 to describe a typical winter (Biggs 1995; see Ballinger 1999). Measurements of average SWE occur at irregular intervals; we used linear interpolation to obtain inputs to the snow model at weekly intervals for a 20-week winter. All of the predicted values, including the timing of the melt, are within the range of historic values but tend toward a mild winter.

A.2 Forage

Vegetation varies considerably over the northern range, and at scales smaller than the size of our patches (Wallace et al., 1995). However, we expect variation in snow to be more important to foraging than variation in vegetation at the scale of the patches. Hence, we assume a constant forage biomass per unit area (1450 kg ha^{-1}) that is within the range of values for different vegetation types measured by Wallace et al. (1995). The total forage available in a patch at the beginning of the winter is equal to the product of this forage density and patch area, which was calculated from GIS data provided by YNP (Ballinger, 1999).

A.3 Hunting

We estimate weekly predation rate outside the park by transforming the average pre-hunt population harvested (9%) into a weekly rate and dividing by the average percent of elk leaving the park (17%). We obtain a weekly per capita predation rate of 2.77%, or $S(p) = 0.9733$ in patches outside the park. These estimates are based on data from 1981-1988 (Singer, 1990).

A.4 Elk energetics

Change in mass is calculated for the one-week time step from the energy balance (Eq. 1). We assume a constant conversion of energy to change in body mass (Torbit et al. 1985, Hobbs 1989). The value of the conversion coefficient (η) accounts for the different rate of mass loss in fat and lean tissue as well as the different energy produced by catabolizing fats and proteins. Similarly, we assume a constant energy content of forage on the Northern Range (Turner et al., 1994), ϵ , in Eq. 8.

The maintenance rate (μ) in Eq. 2 differs between calves and adults (Thompson et al., 1973). The values listed in Table 2 are based on continuous change in mass with time; however, because body mass changes slowly, this approximation is reasonable for the one-week time step used in the dynamic programming algorithm.

Travel cost is an increasing function of mass and snow depth (Parker et al., 1984). The value of K in Eq. 3 is the total distance traveled. Eq. 3 applies to horizontal movement; we do not model movement at sufficiently small scale to estimate uphill and downhill travel. Parker et al. (1984) derived an empirical relationship between the relative sinking depth and the increase in travel costs due to snow, where relative sinking depth is given as a percent of brisket height. For simplicity, we set relative sinking depth equal to the snow depth. In crusted or dense snow, this approximation is inaccurate (Bunnell et al., 1990) and effectively increases the severity of the

winter in our model.

The distance traveled consists of two parts: movement for daily activity and movement between patches. Turner et al. (1994) estimate that, not including the larger scale movement, elk move on average about 4 km per day. Hence, to obtain K , we add 28 km to the distance traveled between patches in each one-week time step.

We assume starvation occurs when mass falls below a threshold value, m_{crit} . Empirical observations suggest that the threshold is loss of 70% of fat mass and 30% of lean mass (Coughenour, 1994; Hobbs, 1989; Turner et al., 1994). Our model does not distinguish fat and lean masses. Using available estimates of body fat percentage (Table 2) at the beginning of winter, we approximate the starvation threshold as 63.6% average initial mass for calves, cows, and bulls.

References

- Alonzo, S. H., & M. Mangel. 2001. Survival strategies and growth of krill: avoiding predators in space and time. *Marine Ecology Progress Series* **209**, 203–217.
- Bailey, D. W., J. E. Gross, E. A. Laca, L. R. Rittenhouse, M. B. Coughenour, D. M. Swift, & P. L. Sims. 1996. Mechanisms that result in large herbivore grazing distribution patterns. *Journal of Range Management* **49**, 386–400.
- Ballinger, L. A., 1999. Yellowstone Elk Migration: A Dynamic Programming Model. Master's thesis, University of Utah.
- Bernstein, C., A. Kacelnik, & J. R. Krebs. 1988. Individual decisions and the distribution of predators in a patchy environment. *Journal of Animal Ecology* **57**, 1007–1026.
- Bernstein, C., A. Kacelnik, & J. R. Krebs. 1991. Individual decisions and the distribution of predators in a patchy environment. II. The influence of travel costs and structure of the environment. *Journal of Animal Ecology* **60**, 205–225.
- Biggs, T., 1995. The development and use of a geographic information systems snow map for estimating equilibrium numbers of the gray wolf in Yellowstone National Park. Honors thesis, Princeton University.
- Bowler, D. E., & T. G. Benton. 2005. Causes and consequences of animal dispersal strategies: relating individual behaviour to spatial dynamics. *Biological Reviews* **80**, 205–225.
- Brown, J. S. 1988. Patch use as an indicator of habitat preference, predation risk, and competition. *Behavioral Ecology and Sociobiology* **22**, 37–47.

- Bunnell, F. L., F. W. Hovey, R. S. McNay, & K. L. Parker. 1990. Forest cover, snow conditions, and black-tailed deer sinking depths. *Canadian Journal of Zoology* **68**, 2403–2408.
- Charnov, E. L. 1976. Optimal foraging, the marginal value theorem. *Theoretical Population Biology* **9**, 129–136.
- Coughenour, M. B. 1991. Spatial components of plant-herbivore interactions in pastoral, ranching, and native ungulate ecosystems. *Journal of Range Management* **44**, 530–542.
- Coughenour, M. B., 1994. Elk carrying capacity on Yellowstone's northern elk winter range: Preliminary modeling to integrate climate, landscape, and nutritional requirements. Pages 97–111 *in* D. Despain, editor. *Plants and their Environments: Proceedings of the First Biennial Scientific Conference on the Greater Yellowstone Ecosystem*.
- Creel, S., J. J. Winnie, B. Maxwell, K. Hamlin, & M. Creel. 2005. Elk alter habitat selection as an antipredator response to wolves. *Ecology* **86**, 3387–3397.
- Emlen, J. 1966. The role of time and energy in food preference. *American Naturalist* **100**, 611–617.
- Farnsworth, K. D., & J. A. Beecham. 1999. How do grazers achieve their distribution? A continuum of models from random diffusion to the ideal free distribution using biased random walks. *American Naturalist* **153**, 509–526.
- Fortin, D., H. L. Beyer, M. Boyce, D. W. Smith, & J. S. Duchesne, Thierry and Mao. 2005*a*. Wolves influence elk movements: behavior shapes a trophic cascade in Yellowstone National Park. *Ecology* **86**, 1320–1330.
- Fortin, D., J. Morales, & M. S. Boyce. 2005*b*. Elk winter foraging at fine scale in Yellowstone National Park. *Behavioural Ecology* **145**, 335–343.

- Fretwell, S. D., & H. L. Lucas. 1970. On territorial behaviour and other factors influencing habitat distribution in birds. I. Theoretical development. *Acta Biotheoretica* **19**, 16–36.
- Grimm, V. 1999. Ten years of individual-based modelling in ecology: what have we learned and what could we learn in the future? *Ecological Modelling* **115**, 129–148.
- Grimm, V., & S. F. Railsback. 2005. *Individual-Based Modeling and Ecology*. Princeton University Press, Princeton, NJ.
- Heinz, S. K., & E. Strand. 2006. Adaptive patch searching strategies in fragmented landscapes. *Evolutionary Ecology* **20**, 113–130.
- Hobbs, N. T. 1989. Linking energy balance to survival in mule deer: Development and test of a simulation model. *Wildlife Monographs* **101**.
- Houston, D. B. 1982. *The Northern Yellowstone Elk*. MacMillan Publishing Co., Inc., New York.
- Huse, G., & J. Giske. 1998. Ecology in Mare Pentium: an individual-based spatio-temporal model for fish with adapted behaviour. *Fisheries Research* **37**, 163–178.
- Jager, H., E. Carr, & R. Efraymson. 2006. Simulated effects of habitat loss and fragmentation on a solitary mustelid predator. *Ecological Modelling* **191**, 416–430.
- Jepsen, J., J. Baveco, C. Topping, J. Verboom, & C. Vos. 2005. Evaluating the effect of corridors and landscape heterogeneity on dispersal probability: a comparison of three spatially explicit modelling approaches. *Ecological Modelling* **181**, 445–459.
- Jonzén, N., C. Wilcox, & H. P. Possingham. 2004. Habitat selection and population regulation in temporally fluctuating environments. *American Naturalist* **164**, E103–E114.

- Lima, S. L., & P. A. Zollner. 1996. Towards a behavioral ecology of ecological landscapes. *Trends in Ecology and Evolution* **11**, 131–135.
- MacArthur, R. H., & E. R. Pianka. 1966. On optimal use of a patchy environment. *American Naturalist* **100**, 603–609.
- Mangel, M., & C. W. Clark. 1988. *Dynamic modeling in behavioral ecology*. Princeton University Press, Princeton, NJ.
- McNamara, J. M., J. N. Webb, E. J. Collins, T. Szekely, & A. I. Houston. 1997. A general technique for computing evolutionarily stable strategies based on errors in decision-making. *Journal of Theoretical Biology* **189**, 211–225.
- Morris, D. W. 2003. Toward an ecological synthesis: a case for habitat selection. *Oecologia* **136**, 1–13.
- National Research Council. 2002. *Ecological Dynamics on Yellowstone's Northern Range*. National Academy Press, Washington, D.C.
- Parker, K. L., C. T. Robbins, & T. A. Hanley. 1984. Energy expenditures for locomotion by mule deer and elk. *Journal of Wildlife Management* **48**, 474–488.
- Revilla, E., T. Wiegand, F. Palomares, P. Ferreras, & M. Delibes. 2004. Effects of matrix heterogeneity on animal dispersal: From individual behavior to metapopulation-level parameters. *American Naturalist* **164**, E130–E153.
- Ripple, W. J., & R. L. Beschta. 2004. Wolves and the ecology of fear: can predation risk structure ecosystems? *Bioscience* **54**, 755–766.

- Senft, R. L., M. B. Coughenour, D. W. Bailey, L. R. Rittenhouse, O. E. Sala, & D. M. Swift. 1987. Large herbivore foraging and ecological hierarchies. *BioScience* **37**, 789–799.
- Singer, F. J., 1990. The ungulate prey base for wolves in Yellowstone National Park I: Five species on the northern range, elk parkwide. Technical report, National Park Service, Division of Research.
- Stephens, D. W., & J. R. Krebs. 1986. *Foraging Theory*. Princeton University Press, Princeton.
- Stephens, P., F. Frey-Roos, W. Arnold, & W. Sutherland. 2002. Model complexity and population predictions. The alpine marmot as a case study. *Journal of Animal Ecology* **71**, 343–361.
- Sutherland, W. J. 1983. Aggregation and the ‘ideal free’ distribution. *Journal of Animal Ecology* **52**, 821–828.
- Sweeney, J. M., & J. R. Sweeney. 1984. Snow depths influencing winter movements of elk. *Journal of Mammalogy* **65**, 524–526.
- Thompson, C. B., J. B. Holter, H. Hayes, H. Silver, & W. E. Urban. 1973. Nutrition of white-tailed deer. I. Energy requirements of fawns. *Journal of Wildlife Management* **37**, 301–311.
- Torbit, S. C., L. H. Carpenter, D. M. Swift, & A. W. Alldredge. 1985. Differential loss of fat and protein by mule deer during winter. *Journal of Wildlife Management* **49**, 80–85.
- Turner, M. G., Y. Wu, W. H. Romme, & L. L. Wallace. 1993. A landscape simulation model of winter foraging by large ungulates. *Ecological Modelling* **69**, 163–184.
- Turner, M. G., Y. Wu, L. L. Wallace, W. H. Romme, L. L. Wallace, & A. Brenkert. 1994.

Simulating winter interactions among ungulates, vegetation, and fire in northern Yellowstone Park. *Ecological Applications* **4**, 472–496.

Wallace, L., M. Turner, W. Romme, R. O'Neill, & Y. Wu. 1995. Scale of heterogeneity of forage production and winter foraging by elk and bison. *Landscape Ecology* **10**, 75–83.

Table 1: Summary of models with (+) and without (-) frequency-dependence (FD) and mass-dependence (MD).

| Model | FD | MD | Quantity maximized |
|-------|----|----|--|
| 1 | - | - | Immediate payoff in the absence of forage depletion by competitors |
| 2 | + | - | Immediate payoff with forage depletion by competitors |
| 3 | - | + | Net payoff in the absence of forage depletion by competitors |
| 4 | + | + | Net payoff with forage depletion by competitors |

Table 2: Parameter values for forage characteristics and elk age/sex classes (see Appendix A).

| Parameter | value | | |
|--|-----------------------|------------|-------------|
| Energy to mass conversion, η (kg kJ ⁻¹) | 7.19×10^{-5} | | |
| Forage energy content, ε (kJ kg ⁻¹) | 5648 | | |
| Minimum unavailable forage fraction, r | 0.13 | | |
| | <i>Calf</i> | <i>Cow</i> | <i>Bull</i> |
| Lower snow threshold, $SW E_{low}$ (cm) | 5 | 5 | 5 |
| Upper snow threshold, $SW E_{high}$ (cm) | 15 | 15 | 15 |
| Maintenance rate, μ (J kg ^{-3/4} week ⁻¹) | 3570 | 2926 | 2926 |
| Brisket height, H (cm) | 72 | 78 | 83 |
| Initial average body fat (% mass) | 8 | 16 | 15 |
| Initial herd size | 2400 | 9900 | 2700 |
| Maximum ingestion rate, I_{max} (kg week ⁻¹) | 3.48 | 4.48 | 5.90 |
| Starvation threshold, m_{crit} (kg) | 107 | 150 | 201 |
| Average mass (kg) | 116 | 179 | 236 |
| Maximum mass, m_{max} (kg) | 127 | 196 | 259 |

Table 3: Predicted winter survival and fraction of forage consumed for optimization models with (+) and without (-) frequency-dependence (FD) and mass-dependence (MD).

| Model | FD | MD | Fraction surviving | | | Forage consumed |
|-------|----|----|--------------------|------|-------|-----------------|
| | | | Calves | Cows | Bulls | |
| 1 | - | - | 0 | 0.98 | 0.98 | 0.0315 |
| 2 | - | + | 0 | 0.96 | 0.99 | 0.0352 |
| 3 | + | - | 0.01 | 0.98 | 0.97 | 0.0290 |
| 4 | + | + | 0.38 | 0.98 | 1.0 | 0.0358 |

Figure legends

Figure 1. Winter range of the northern Yellowstone elk herd with ungulate count unit (patch) boundaries and numbers. Dash-dotted line indicates YNP boundary.

Figure 2. Sample output from the full model. Upper panel: each arrow indicates movement of more than 100 elk at any time step during the entire winter. Movement of smaller numbers of elk occurs from all patches, but arrows are not displayed for clarity. Lower panel: density of elk at the end of week 5 (darker shading indicates higher density).

Figure 3. Predictions for herd distribution from the four models: base model (model 1, solid lines), frequency-dependence without mass-dependence (model 2, dotted lines), mass-dependence without frequency-dependence (model 3, dashed lines), and the full dynamic game (model 4, dot-dash lines). a) Use of habitat outside YNP. b) Aggregation among all patches, measured by the coefficient of variation (CV).

Figure 4. Optimal behavior of the herd for model 1 is approximately the same for all age/sex classes (dotted lines show cow distribution; calf-cow pair and bull distributions are indistinguishable). Predictions for the optimization model with state dependence (model 2, solid lines) differ for cow-calf pairs (circles), cows (squares), and bulls (triangles). a) Fraction of the herd in patches outside YNP. b) Distribution of the herd among all patches. Increasing coefficient of variation (CV) indicates increasing aggregation in fewer patches.

Figure 5. Predicted distribution of the herd for three models: optimization without state-dependence (model 1, dotted line), ideal free distribution with travel costs (model 2, crosses), and the full state-dependent game (model 4, diamonds).

Figure 6. Predictions for the full model (dotted lines) and the full model with heterogeneity in snow within patches. 10% of the forage in each patch is located in areas with snow accumulation

predicted for the minimum elevation in the patch. Elk in a given patch consume the forage from the area with less snow first, before grazing in areas with deeper snow. a) Fraction of the herd in patches outside YNP, and b) distribution of the herd among all patches, for calf-cow pairs (circles), cows (squares), and bulls (triangles).

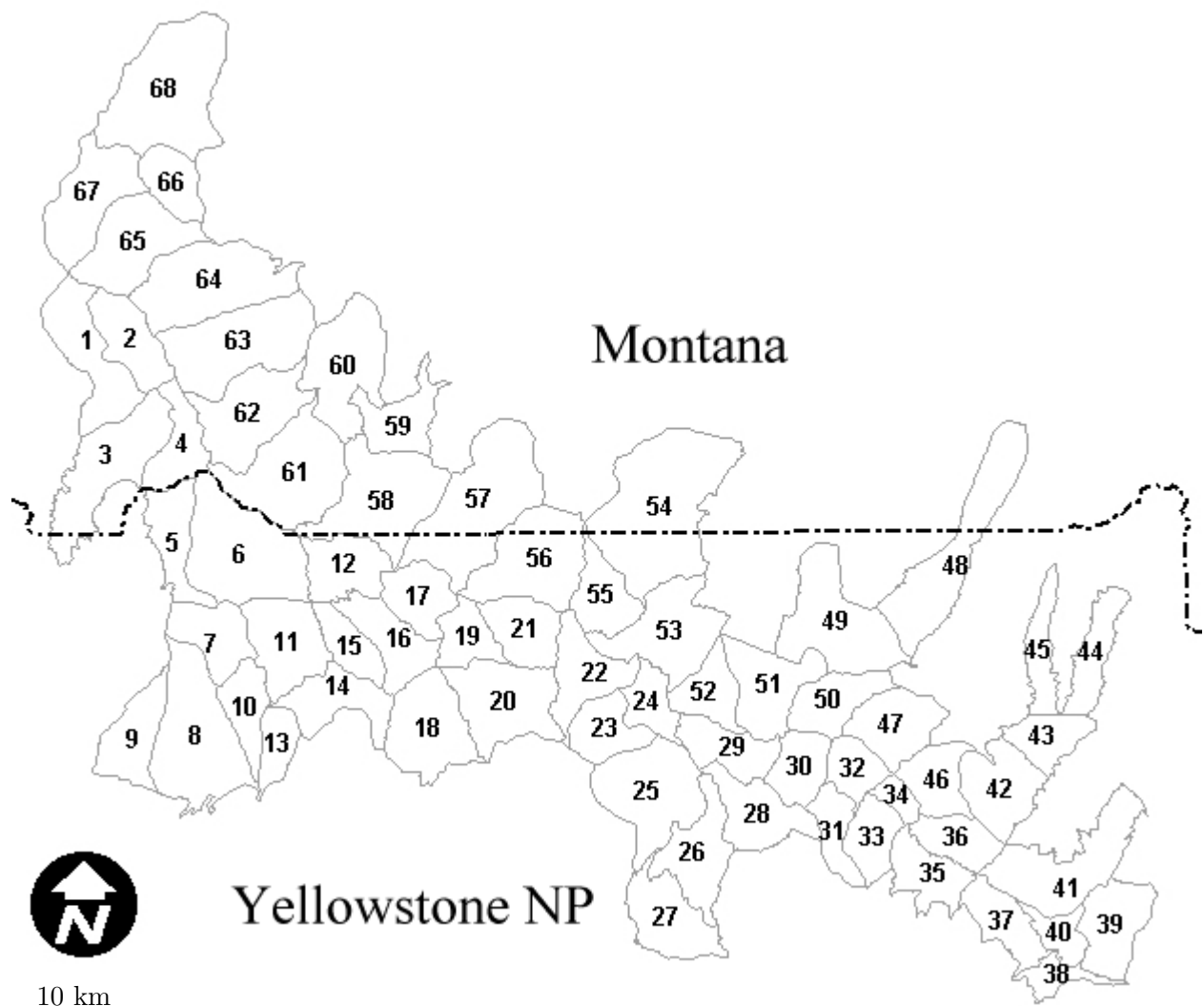


Figure 1: Winter range of the northern Yellowstone elk herd with NPS count unit (patch) boundaries and numbers. Dash-dotted line indicates YNP boundary.

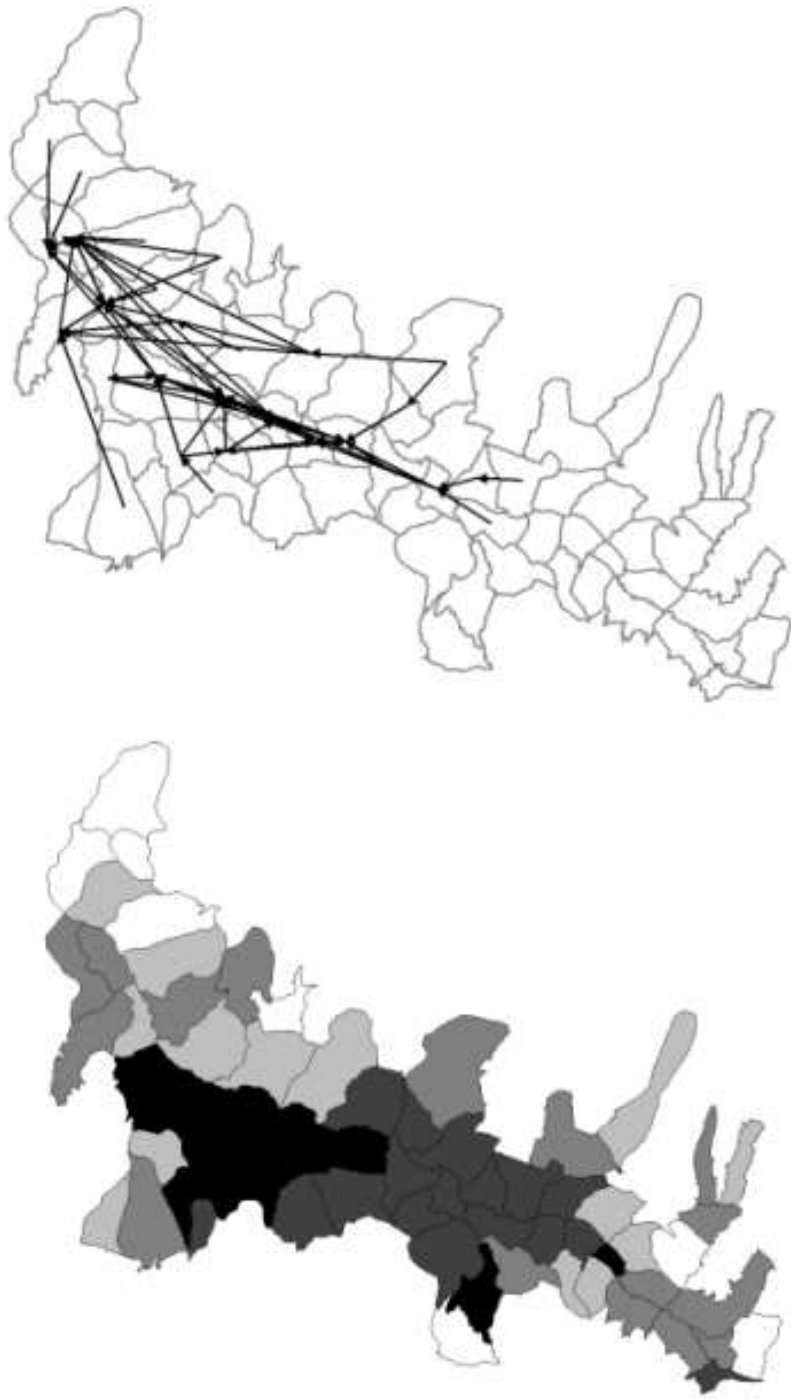


Figure 2: Sample output from the full model. Upper panel: each arrow indicates movement of more than 100 elk at any time step during the entire winter. Movement of smaller numbers of elk occurs from all patches, but arrows are not displayed for clarity. Lower panel: density of elk at the end of week 5 (darker shading indicates higher density).

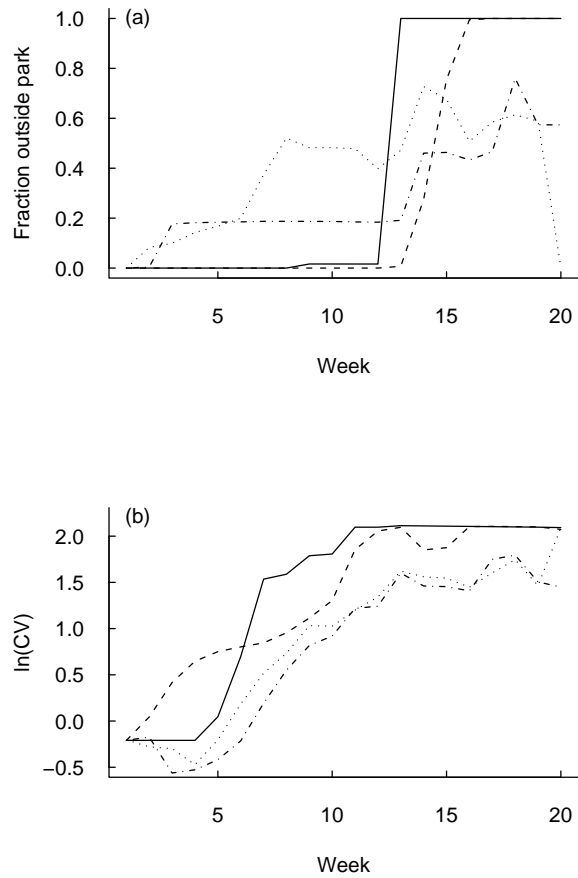


Figure 3: Predictions for herd distribution from the four models: base model (solid lines), frequency dependence without mass dependence (dotted lines), mass dependence without frequency dependence (dashed lines), and the full model (dot-dash lines). a) Use of habitat outside YNP. b) Aggregation among all patches, measured by the coefficient of variation (CV).

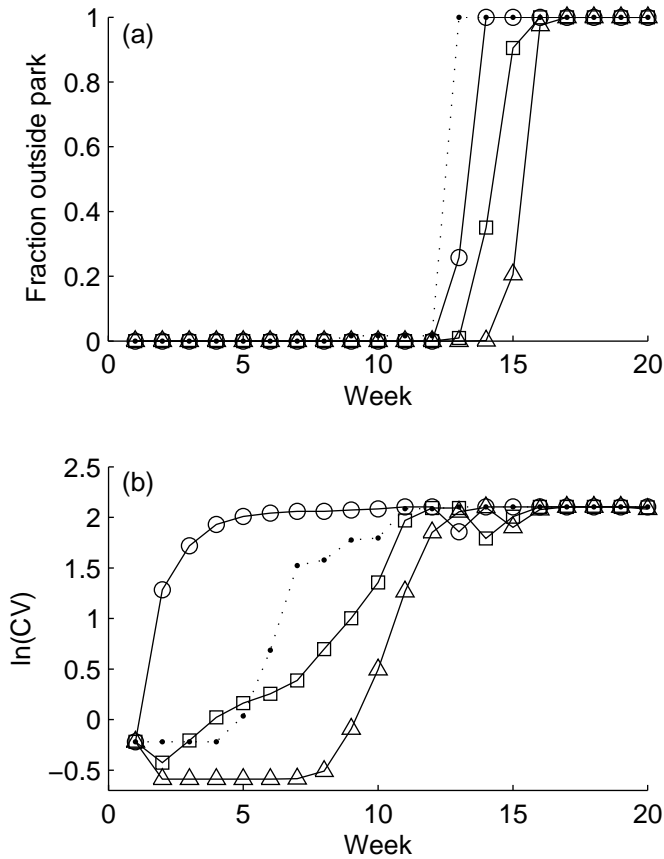


Figure 4: Optimal behavior of the herd for model 1 is approximately the same for all age/sex classes (dotted lines show cow distribution; calf-cow pair and bull distributions are indistinguishable). Predictions for the optimization model with state dependence (model 2, solid lines) differ for cow-calf pairs (circles), cows (squares), and bulls (triangles). a) Fraction of the herd in patches outside YNP. b) Distribution of the herd among all patches. Increasing coefficient of variation (CV) indicates increasing aggregation in fewer patches.

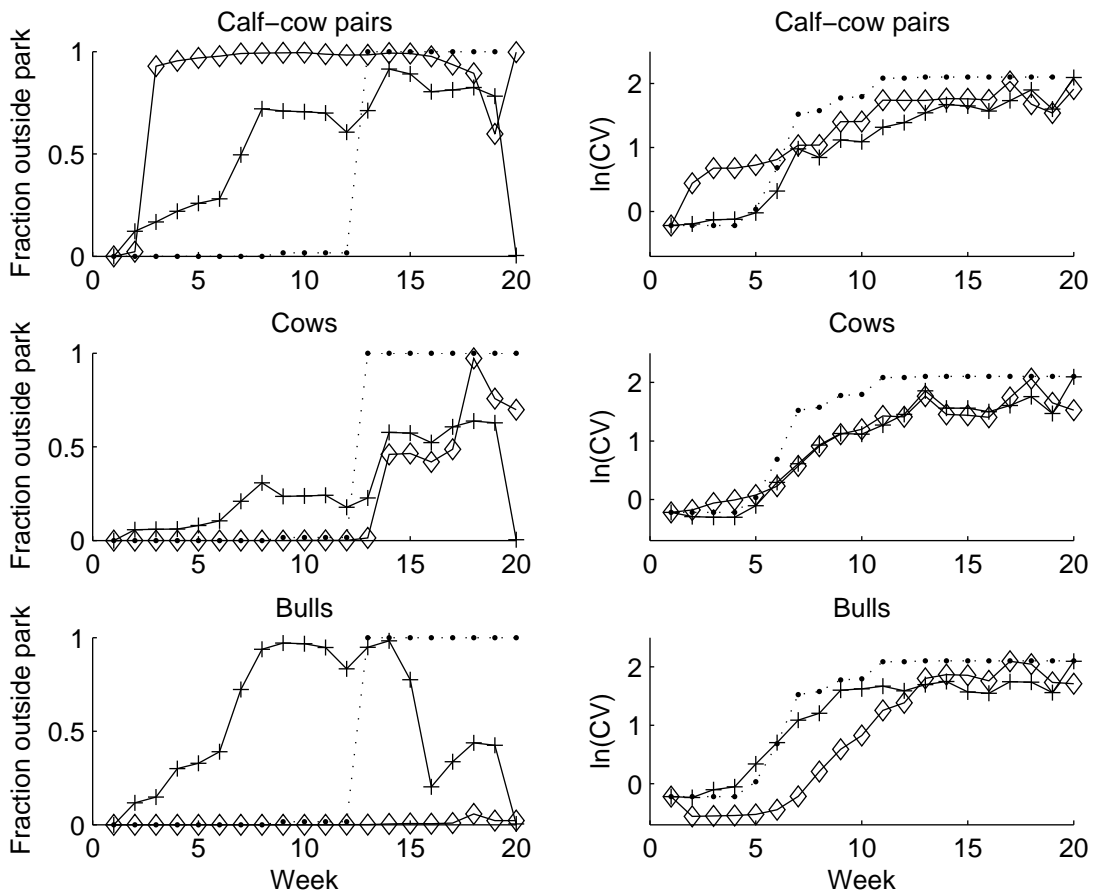


Figure 5: Predicted distribution of the herd for three models: optimization without state-dependence (model 1, dotted line), ideal free distribution with travel costs (model 2, crosses), and the full state-dependent game (model 4, diamonds).

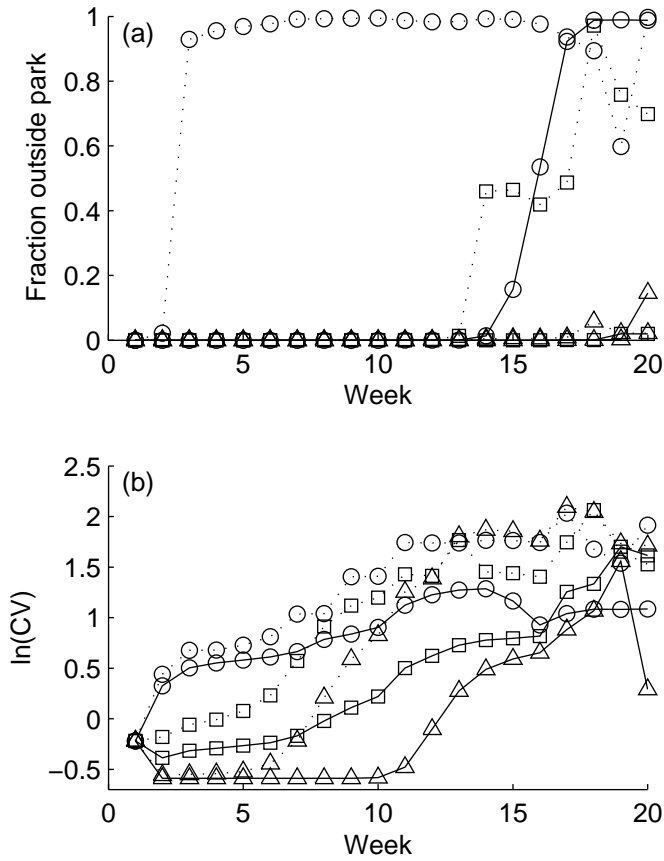


Figure 6: Predictions for the full model (dotted lines) and the full model with heterogeneity in snow within patches. 10% of the forage in each patch is located in areas with snow accumulation predicted for the minimum elevation in the patch. Elk in a given patch consume the forage from the area with less snow first, before grazing in areas with deeper snow. a) Fraction of the herd in patches outside YNP, and b) distribution of the herd among all patches, for calf-cow pairs (circles), cows (squares), and bulls (triangles).